

Article

Mechanism of Nitrite Formation by Nitrate Photolysis in Aqueous Solutions: The Role of Peroxynitrite, Nitrogen Dioxide, and Hydroxyl Radical

Sara Goldstein, and Joseph Rabani

J. Am. Chem. Soc., **2007**, 129 (34), 10597-10601 • DOI: 10.1021/ja073609+ • Publication Date (Web): 04 August 2007

Downloaded from <http://pubs.acs.org> on March 19, 2009

More About This Article

Additional resources and features associated with this article are available within the HTML version:

- Supporting Information
- Links to the 5 articles that cite this article, as of the time of this article download
- Access to high resolution figures
- Links to articles and content related to this article
- Copyright permission to reproduce figures and/or text from this article

[View the Full Text HTML](#)



ACS Publications
High quality. High impact.

Mechanism of Nitrite Formation by Nitrate Photolysis in Aqueous Solutions: The Role of Peroxynitrite, Nitrogen Dioxide, and Hydroxyl Radical

Sara Goldstein* and Joseph Rabani

Contribution from the Department of Physical Chemistry, The Hebrew University of Jerusalem, Jerusalem 91904, Israel

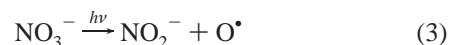
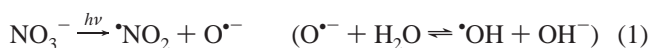
Received May 20, 2007; E-mail: sarag@vms.huji.ac.il

Abstract: Photolysis of aqueous NO_3^- with $\lambda \geq 195$ nm is known to induce the formation of NO_2^- and O_2 as the only stable products. The mechanism of NO_3^- photolysis, however, is complex, and there is still uncertainty about the primary photoprocesses and subsequent reactions. This is, in part, due to photoisomerization of NO_3^- to ONOO^- at $\lambda < 280$ nm, followed by the formation of $\cdot\text{OH}$ and $\cdot\text{NO}_2$ through the decomposition of ONOOH ($\text{p}K_a = 6.5\text{--}6.8$). Because of incomplete information concerning the mechanism of peroxynitrite ($\text{ONOOH}/\text{ONOO}^-$) decomposition, previous studies were unable to account for all observations. In the present study aqueous nitrate solutions were photolyzed by monochromatic light in the range of 205–300 nm. It is shown that the main primary processes at this wavelength range are $\text{NO}_3^- \xrightarrow{h\nu} \cdot\text{NO}_2 + \text{O}^{\cdot-}$ (reaction 1) and $\text{NO}_3^- \xrightarrow{h\nu} \text{ONOO}^-$ (reaction 2). Based on recent knowledge on the mechanisms of peroxynitrite decomposition and its reactions with reactive nitrogen and oxygen species, we determined $\Phi(1)$ and $\Phi(2)$ using different experimental approaches. Both quantum yields increase with decreasing the excitation wavelength, approaching $\Phi(1) = 0.13$ and $\Phi(2) = 0.28$ at 205 nm. It is also shown that the yield of nitrite increases with decreasing the excitation wavelength. The implications of these results on UV disinfection of drinking water are discussed.

Introduction

It is well-known that the overall stable products resulting from the photolysis of aqueous NO_3^- at $\lambda \geq 195$ nm are NO_2^- and O_2 .^{1–3} The mechanism of NO_3^- photolysis is complex, and there is still uncertainty about the primary photoprocesses and subsequent reactions.^{3–6} This is in part due to the photoisomerization of NO_3^- to ONOO^- and the formation of $\cdot\text{OH}$ and $\cdot\text{NO}_2$ through the decomposition of ONOOH ($\text{p}K_a = 6.5\text{--}6.8$).⁷ Because of incomplete information concerning the mechanism of peroxynitrite ($\text{ONOOH}/\text{ONOO}^-$) decomposition, previous studies were unable to account for all observations. Only recently, with renewed interest in peroxynitrite promoted by its important role in biological systems,^{8,9} has the detailed reaction mechanism been elucidated,⁷ motivating us to revisit this system.

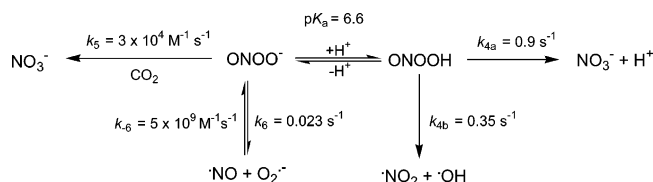
The absorption spectrum of NO_3^- is dominant by a weak $n \rightarrow \pi^*$ band around 302 nm ($\epsilon = 7.2 \text{ M}^{-1} \text{ cm}^{-1}$) and a much stronger $\pi \rightarrow \pi^*$ band at 200 nm ($\epsilon = 9900 \text{ M}^{-1} \text{ cm}^{-1}$). It has been suggested that excitation in the $\pi \rightarrow \pi^*$ band ($\lambda < 280$ nm) proceeds via the two primary photoprocesses 1 and 2, whereas excitation in the $n \rightarrow \pi^*$ band ($\lambda > 280$ nm) proceeds through 1 and 3.³



Flash-photolysis studies at the 200 nm band provide evidence for the formation of ONOO^- , $\cdot\text{NO}_2$, and $\cdot\text{OH}$.^{1,2} However, a recent femtosecond transient absorption spectroscopy shows the formation of ONOO^- with $\Phi = 0.48$ and $[\text{NO} + \text{O}_2]^-$ with $\Phi = 0.08$ within 2 ps.⁶ This suggests that $\cdot\text{NO}_2$, observed in the flash photolysis, is produced by subsequent reactions.

In any case, the main contribution to nitrite formation at $\lambda < 280$ nm is through the decomposition of peroxynitrite. ONOOH decays almost entirely into nitrate with $k_d = 1.25 \pm 0.05 \text{ s}^{-1}$ at 25 °C,^{10,11} whereas ONOO^- is relatively stable. Upon increasing the pH, nitrite and O_2 at a ratio 2:1 are formed at the expense of nitrate. At pH 9–10 the yield of nitrite amounts to about 80% of the initial peroxynitrite.^{12–14} These results can be

- (1) Shuali, H.; Ottolenghi, M.; Rabani, J.; Yelin, Z. *J. Phys. Chem.* **1969**, *73*, 3445–3451.
- (2) Barat, F.; Gilles, L.; Hickel, B.; Sutton, J. *J. Chem. Soc. A* **1970**, 1982–1986.
- (3) Mack, J.; Bolton, J. R. *J. Photochem. Photobiol., A* **1999**, *128*, 1–13.
- (4) Mark, G.; Korth, H.-G.; Schuchmann, H.-P.; von Sonntag, C. *J. Photochem. Photobiol., A* **1996**, *101*, 89–103.
- (5) Sharpless, C. M.; Linden, K. G. *Environ. Sci. Technol.* **2001**, *35*, 2949–2955.
- (6) Madsen, D.; Larsen, J.; Jensen, S. K.; Keiding, S. R.; Thøgersen, J. *J. Am. Chem. Soc.* **2003**, *125*, 15571–15576.
- (7) Goldstein, S.; Lind, J.; Merenyi, G. *Chem. Rev.* **2005**, *105*, 2457–2470.
- (8) Beckman, J. S.; Beckman, T. W.; Chen, J.; Marshall, P. A.; Freeman, B. A. *Proc. Natl. Acad. Sci. U.S.A.* **1990**, *87*, 1620–1624.
- (9) Radi, R.; Peluffo, G.; Alvarez, M. N.; Naviliat, M.; Cayota, A. *Free Radical Biol. Med.* **2001**, *30*, 463–488.

Scheme 1. Primary Reactions during Peroxynitrite Decomposition in the Absence and Presence of CO_2^a 

^a All rate constants are taken from ref 7 except k_5 (ref 16).

rationalized by assuming the homolysis of ONOOH and homolytic equilibrium of ONOO⁻ (Scheme 1) followed by subsequent radical reactions (not shown in Scheme 1), e.g., the reaction of $\cdot\text{OH}$ with ONOO⁻ and NO₂⁻, the reaction of $\cdot\text{NO}_2$ with O₂⁻ and $\cdot\text{NO}$, hydrolysis of $\cdot\text{NO}_2$. Evidently, the overall rates of the different reaction paths strongly depend on the experimental conditions.⁷

The homolytic equilibrium between ONOO⁻ and $\cdot\text{NO} + \text{O}_2^-$ has not yet been considered as an important reaction pathway during the photolysis of NO₃⁻. This homolytic equilibrium contributes to the yield of nitrite since the reaction of $\cdot\text{NO}_2$ with $\cdot\text{NO}$ forms N₂O₃, which hydrolyzes to NO₂⁻, and that with O₂⁻ produces O₂NOO⁻, which decomposes into NO₂⁻ and O₂.¹⁵ The formation of $\cdot\text{OH}$ radicals both by the photolysis of NO₃⁻ and decomposition of ONOOH makes the system sensitive to the presence of organic impurities, as most organic materials react efficiently with $\cdot\text{OH}$. Further complication results when the solutions are contaminated with CO₂, which lowers the nitrite yield by catalyzing the decomposition of ONOO⁻ into NO₃⁻ (Scheme 1, reaction 5).^{16,17}

In the present study we determined $\Phi(1)$ and $\Phi(2)$ in nitrate solutions excited by monochromatic light in the range of 205–300 nm using different experimental approaches, which take into consideration the complexity of the system as described above and in more detail in a recent review.⁷ The implications of the present results on UV disinfection of drinking water are also discussed.

Experimental Section

Materials. All chemicals were of the highest available purity. Solutions were prepared with deionized water, which was treated using a Milli-Q water purification system. Nitrate solutions were prepared by dissolving the appropriate amount of NaNO₃ (Merck 99.5%) and NaH₂PO₄ (Mallinckrodt 99.9%), and the pH was adjusted with solutions of HClO₄ (J. T. Baker 69–72%) or NaOH (1 M, J. T. Baker). The Griess reagent (modified) was purchased from Sigma.

Analysis. The concentration of peroxynitrite was determined from its absorption using $\epsilon_{302} = 1670 \text{ M}^{-1} \text{ cm}^{-1}$.¹⁸ The concentration of nitrite was determined by mixing equal volumes of the sample and the Griess reagent. The absorption at 540 nm was read after 15 min against nonirradiated sample. Calibration was carried out using aqueous

solutions containing known concentrations of nitrite. Formaldehyde was determined using the Nash reagent (2 M ammonium acetate, 0.05 M acetic acid, 0.02 M acetylacetone).¹⁹ The reagent was mixed with an equal volume of the tested solution, and after incubation for about 15 min at 50 °C, the concentration of formaldehyde was determined from its absorption using $\epsilon_{412} = 8000 \text{ M}^{-1} \text{ cm}^{-1}$.¹⁹

Photolysis. Irradiations were carried out in cylindrical cells (2 cm i.d., 1 or 2 cm length) made from Suprasil quartz under magnetic stirring at room temperature (24 ± 1 °C). The light entered through a flat optical window. The 1 cm long cell was used with the xenon light source, and the 2 cm long cell was used with the mercury lamp. The cells had short side arms with glass taper joints, through which the solutions were introduced. A small stirrer was placed in the solutions outside the light path. The volumes of the illuminated solutions (including a small amount in the side arms, corrected for the stirrer) were measured as 3.07 and 6.67 mL, respectively. This was calculated from the difference in the weight of the cell, stirrer, and stopper with and without water. Two light sources were used: (i) A monochromatic low-pressure mercury lamp (Heraeus NNI 120/44U, with the 185 nm line filtered out). The monochromatic light passed through a 10 cm long tube located between the lamp and the sample. The incident light intensity was controlled by changing the distance between the lamp and the sample. (ii) A xenon lamp (Osram 150 W ozone-free) coupled with a monochromator (SX-17MV setup from Applied Photophysics).

The incident light density was measured with a calibrated Si photosensor (Hamamatsu S2281) coupled with a Keithley 617 programmable electrometer and by the iodide–iodate actinometer.²⁰ An iodide–iodate actinometer was daily prepared. It contained 0.6 M potassium iodide and 0.1 M potassium iodate in 0.01 M Na₂B₄O₇·12 H₂O, at pH 9.25 (all three products of Sigma-Aldrich, reagent grade). We have recently redetermined the quantum yields of I₃⁻, and the values used in the present study are 0.92 at 205–240 nm, 0.72 at 253.7 nm, 0.53 at 260 nm, 0.42 at 270 nm, and 0.28 at 300 nm.²¹ Direct measurements of scattered light was done by comparing between the light signal at a given wavelength to that observed when the monochromator is set to 170 nm (where the light intensity is practically zero). This showed only 0.6% scattered light at 300 nm increasing to about 13% at 205 nm. Using the photosensor, the absorbed light was corrected for the scattered light and also by 4%, which accounts for the reflection of the incident light from the surface of the quartz cell. No corrections were done using the iodide–iodate actinometer as it is assumed that scattered light is from long wavelengths where both aqueous nitrate and iodide–iodate actinometer solutions are optically transparent. This assumption was verified using narrow band interference filters (10–12 nm) at 205 and 214 nm with 14% and 22% peak transmittance, respectively. The light absorbed by nitrate solutions was calculated using Beer's law. Modeling of the experimental results was carried out using INTKIN, a noncommercial program developed at Brookhaven National Laboratories by Dr. H. A. Schwarz.

Results and Discussion

The apparent rate constants of the decay of ONOO⁻ are 3.2×10^{-5} and $1.3 \times 10^{-5} \text{ s}^{-1}$ at pH 12 and 13, respectively, at 25 °C, independent of peroxynitrite concentration.¹¹ Hence, the half-life of ONOO⁻ at pH ≥ 12 is longer than 6 h enabling its accurate detection within less than 10 min of radiation. 2-Propanol (20 mM) was added to the alkaline nitrate to protect ONOO⁻ from its reaction with $\cdot\text{OH}$. 2-Propanol was chosen as an $\cdot\text{OH}$ scavenger because in aerated solutions the products of this reaction are acetone and O₂⁻. Acetone reacts slowly with ONOO⁻, i.e., $k = 0.066$ and 0.02 s^{-1} at pH 12 and 13,

(10) Kissner, R.; Nauser, T.; Bugnon, P.; Lye, P. G.; Koppenol, W. H. *Chem. Res. Toxicol.* **1997**, *10*, 1285–1292.

(11) Merenyi, G.; Lind, J.; Goldstein, S.; Czapski, G. *J. Phys. Chem. A* **1999**, *103*, 5685–5691.

(12) Pfeiffer, S.; Goren, A. C. F.; Schmidt, K.; Werner, E. R.; Hansert, B.; Bohle, D. S.; Mayer, B. *J. Biol. Chem.* **1997**, *272*, 3465–3470.

(13) Kirsch, M.; Korth, H.-G.; Wensing, A.; Sustmann, R.; de Groot, H. *Arch. Biochem. Biophys.* **2003**, *418*, 133–150.

(14) Lymar, S. V.; Khairutdinov, R. F.; Hurst, J. K. *Inorg. Chem.* **2003**, *42*, 5259–5266.

(15) Logager, T.; Sehested, K. *J. Phys. Chem.* **1993**, *97*, 10047–10052.

(16) Lymar, S. V.; Hurst, J. K. *J. Am. Chem. Soc.* **1995**, *117*, 8867–8868.

(17) Uppu, R. M.; Squadrito, G. L.; Pryor, W. A. *Arch. Biochem. Biophys.* **1996**, *327*, 335–343.

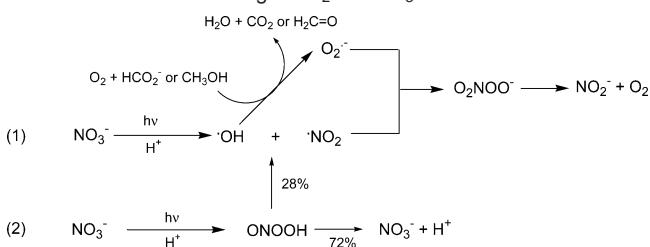
(18) Hughes, M. N.; Nicklin, H. G. *J. Chem. Soc. A* **1968**, 450–452.

(19) Nash, T. *Biochem. J.* **1953**, *55*, 416–421.

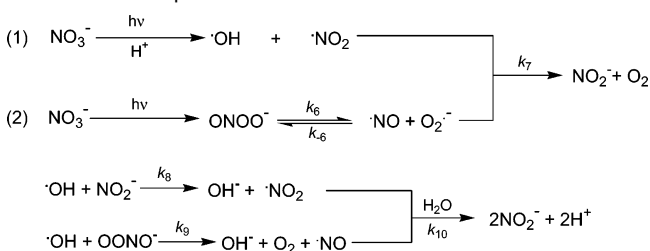
(20) Rahn, R. O.; Stefan, M. I.; Bolton, J. R.; Goren, E.; Shaw, P. S.; Lykke, K. R. *Photochem. Photobiol.* **2003**, *78*, 146–152.

(21) Goldstein, S.; Rabani, J. *J. Photochem. Photobiol.*, in press, 2007.

Scheme 2. Reaction Mechanism for the Production of NO_2^- in Acidic Solutions Containing HCO_2^- or CH_3OH



Scheme 3. Mechanism of Peroxynitrite Decomposition in the Absence of 2-Propanol



respectively,²² while no measurable reaction of $\text{O}_2^{\cdot-}$ with ONOO^- has been reported. Although carbonate is usually present as a contaminant in alkaline solutions, it has no effect on the decomposition of peroxynitrite because the concentration of the active form CO_2 at $\text{pH} \geq 12$ is negligible. Hence, under these conditions $\Phi(\text{ONOO}^-)_{2\text{-propanol}} = \Phi(2)$.

The total quantum yield of the $\cdot\text{OH}$ radical, produced both by the decomposition of peroxynitrite and as a possible primary product, was determined by measuring the formation yield of NO_2^- in the presence of HCO_2Na or CH_3OH in acidic solutions. Under such conditions, the reactions of HCO_2^- with peroxynitrite is relatively slow²³ and does not compete with the self-decomposition of peroxynitrite. Although the reaction of $\cdot\text{OH}$ with HCO_2^- in aerated solutions forms $\text{O}_2^{\cdot-}$ and CO_2 , the latter reacts fast only with ONOO^- ,¹⁶ and therefore it does not affect the yield of NO_2^- . The reaction of $\cdot\text{OH}$ with CH_3OH in aerated solutions forms $\text{O}_2^{\cdot-}$ and $\text{H}_2\text{C}=\text{O}$. As will be shown below, the reaction of $\text{H}_2\text{C}=\text{O}$ with ONOO^- does not compete with the faster self-decomposition of peroxynitrite at this pH range. The reaction mechanism for the production of NO_2^- in acidic solutions containing HCO_2^- or CH_3OH is described in Scheme 2. Scheme 2 shows that the yield of NO_2^- equals the total yield of $\cdot\text{OH}$. The homolysis of ONOOH produces about 28% $\cdot\text{OH}$ and $\cdot\text{NO}_2$,^{14,24} and therefore, $\Phi(\text{NO}_2^-) = \Phi(1) + 0.28\Phi(2)$. Thus, knowing the values of $\Phi(2) = \Phi(\text{ONOO}^-)_{2\text{-propanol}}$ and $\Phi(\text{NO}_2^-)$ allows the calculation of $\Phi(1)$.

A different experimental approach to determine $\Phi(1)$ is based on measurements of peroxynitrite yield at pH 13 in the presence and absence of 2-propanol.⁴ This approach has the advantage that all the relevant data is at the same pH, whereas in the first approach $\Phi(2)$ measured in alkaline solution is coupled with nitrite measured in acidic solution for the derivation of $\Phi(1)$. The mechanism of peroxynitrite decomposition in the absence of 2-propanol is described in Scheme 3. Each pair of $\cdot\text{OH}$ and $\cdot\text{NO}_2$ produced by reaction 1 destroys one ONOO^- ion irrespective on the distribution of $\cdot\text{OH}$ between reactions 8 and

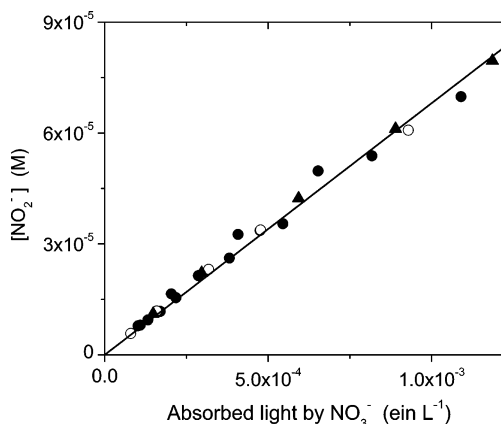


Figure 1. Formation of nitrite upon photolysis of aerated solutions containing (●) 0.1 M NO_3^- , 0.02 M CH_3OH , 0.01 M PB, pH 6.1; (○) 0.02 M NO_3^- , 0.02 M CH_3OH , 0.01 M PB, pH 6.0; (▲) 0.1 M NO_3^- , 0.01 M HCO_2^- , pH 4.7. The absorbed dose rate varied between 1.72×10^{-8} and 1.08×10^{-6} einstein $\text{L}^{-1} \text{s}^{-1}$.

9: If $\cdot\text{OH}$ is converted to $\cdot\text{NO}_2$ by reaction with NO_2^- , the resulting $\cdot\text{NO}_2$ pair destroys one ONOO^- ion through the removal of $\cdot\text{NO}$ and $\text{O}_2^{\cdot-}$ (eq 6). The same result is obtained upon reaction of $\cdot\text{OH}$ with ONOO^- according to eq 8 because the produced $\cdot\text{NO}$ reacts with $\cdot\text{NO}_2$ so that the net effect is the removal of one ONOO^- ion by the $\cdot\text{OH}$ radical. Hence, $\Phi(1) = \Phi(\text{ONOO}^-)_{2\text{-propanol}} - \Phi(\text{ONOO}^-)_{\text{no propanol}}$. Note that if reaction 1 does not take place, as suggested by Madsen et al.,⁶ the yield of peroxynitrite at pH 13 should not be affected by the presence of 2-propanol.

Photolysis at 253.7 nm Using the Low-Pressure Mercury Lamp. The yield of nitrite was determined upon photolysis of aerated aqueous solutions containing 0.02 or 0.1 M NaNO_3 and 0.01 M PB (phosphate buffer). Some of the experiments were carried out in the presence of 0.02 M CH_3OH at pH 5.9–6.2, whereas others were carried out in the presence of 0.01 M HCO_2Na at pH 4.7 yielding similar results (see below). The yield of nitrite was below the detection limit when a cutoff filter, which eliminates the light below 270 nm, was used indicating that the contribution of light from higher wavelengths is negligible. The yield of nitrite was independent of the incident light intensity and NO_3^- concentration. It increased linearly with the absorbed dose yielding the same quantum yield in the presence of HCO_2^- or CH_3OH (Figure 1). From the slope of the line in Figure 1 $\Phi(\text{NO}_2^-) = 0.065 \pm 0.002$ was derived.

In the presence of CH_3OH , $\Phi(\text{NO}_2^-) \approx \Phi(\text{H}_2\text{C}=\text{O})$ implying that under our experimental conditions $\text{H}_2\text{C}=\text{O}$ does not react with peroxynitrite.

The concentration of ONOO^- was measured immediately after photolysis of aerated solutions containing 0.05 or 0.1 M NaNO_3 , 0.02 M 2-propanol, and 0.01 or 0.1 M NaOH . The experiments in the absence of 2-propanol were carried out in the presence of 0.1 M NaNO_3 and 0.1 M NaOH . The concentration of ONOO^- increased linearly with the absorbed dose as demonstrated in Figure 2. The quantum yields of peroxynitrite were determined from the slopes of the lines in Figure 2 as $\Phi(\text{ONOO}^-)_{2\text{-propanol}} = \Phi(2) = 0.102 \pm 0.002$ and $\Phi(\text{ONOO}^-)_{\text{no propanol}} = 0.065 \pm 0.002$. Hence, the first approach, where $\Phi(\text{NO}_2^-) = \Phi(1) + 0.28\Phi(2)$ yields $\Phi(1) = 0.036 \pm 0.004$. The second approach, where $\Phi(1) = \Phi(\text{ONOO}^-)_{2\text{-propanol}} - \Phi(\text{ONOO}^-)_{\text{no propanol}}$, yields almost the same $\Phi(1) = 0.037 \pm 0.004$. Since the first approach is based on measurements of

(22) Merenyi, G.; Lind, J.; Goldstein, S. *J. Am. Chem. Soc.* **2002**, *124*, 40–48.

(23) Goldstein, S.; Czapski, G. *J. Am. Chem. Soc.* **1998**, *120*, 3458–3463.

(24) Hodges, G. R.; Ingold, K. U. *J. Am. Chem. Soc.* **1999**, *121*, 10695–10701.

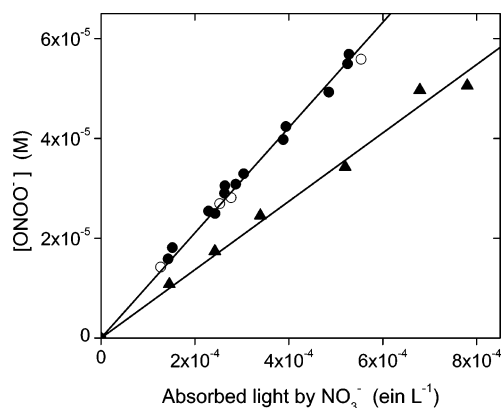


Figure 2. Formation of peroxyntirite formed upon photolysis of aerated solutions containing (●) 0.05 or 0.1 M NO_3^- , 0.02 M 2-propanol, 0.1 M NaOH; (○) 0.05 or 0.1 M NO_3^- , 0.02 M 2-propanol, 0.01 M NaOH; (▲) 0.1 M NO_3^- , 0.1 M NaOH. The absorbed dose rate varied between 8.06×10^{-7} and 1.34×10^{-6} einstein $\text{L}^{-1} \text{s}^{-1}$.

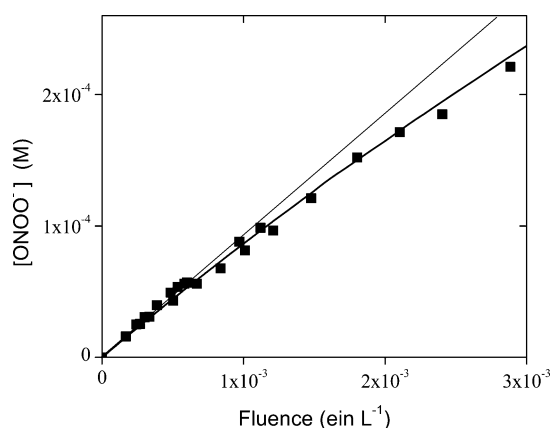


Figure 3. Formation of peroxyntirite upon photolysis of aerated solutions containing 0.1 M NO_3^- , 0.02 M 2-propanol, and 0.1 M NaOH. The incident light intensity varied between 9.3×10^{-7} and 1.16×10^{-6} einstein $\text{L}^{-1} \text{s}^{-1}$. The solid line is the simulated yield of ONOO^- using $\Phi(2) = 0.102$, $\epsilon_{253.7}(\text{ONOO}^-) = 550 \text{ M}^{-1} \text{ cm}^{-1}$, $\epsilon_{253.7}(\text{NO}_3^-) = 4.25 \text{ M}^{-1} \text{ cm}^{-1}$, and $k_d = 1.3 \times 10^{-5} \text{ s}^{-1}$ for the spontaneous decomposition of peroxyntirite.

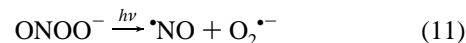
nitrite and peroxyntirite at pH 4.7–6.2 and 13, respectively, whereas the other approach uses data at pH 13, the similar $\Phi(1)$ values indicate that the quantum yields are pH-independent. The similar $\Phi(1)$ also support once again that ONOOH undergoes homolysis forming about 28% $\cdot\text{OH}$ and $\cdot\text{NO}_2$ radicals.

Mark et al.⁴ were unaware of the homolytic equilibrium 6 and therefore assumed that $\Phi(\text{ONOO}^-)_{2\text{-propanol}} - \Phi(\text{ONOO}^-)_{\text{no propanol}}$ represents the lower limit for $\Phi(1)$. They determined experimentally $\Phi(\text{ONOO}^-)_{2\text{-propanol}} = 0.1$ and $\Phi(\text{ONOO}^-)_{\text{no propanol}} = 0.06$ and calculated $\Phi(1) = 0.09$ using $\Phi(\text{Fe}^{2+}) = 1.25$ for the ferrioxalate actinometer. Correction of the $\Phi(\text{ONOO}^-)$ values by using the recently revised $\Phi(\text{Fe}^{2+}) = 1.4$ at 254 nm²¹ yields 0.089 and 0.054, respectively. Hence, $\Phi(1) = 0.089 - 0.054 = 0.035$ is in good agreement with the value reported in the present work.

The buildup of ONOO^- in alkaline solution containing 2-propanol deviates from linearity at relatively high dose as demonstrated in Figure 3, where the straight line corresponds to a constant $\Phi(2) = 0.102$. The deviation from linearity is significantly higher than that expected due to self-decomposition of ONOO^- ($k_d = 1.3 \times 10^{-5} \text{ s}^{-1}$) and its slow reaction with the produced acetone. It is attributed to the absorption of the

light by the accumulated ONOO^- ($\epsilon_{255}(\text{ONOO}^-) \sim 500 \text{ M}^{-1} \text{ cm}^{-1}$).²⁵

The photolysis of ONOO^- results in the formation of $\cdot\text{NO}$ and $\text{O}_2^{\cdot-}$ (reaction 11),¹⁰ which recombine fast back to ONOO^- (eq 6), so that the net role of ONOO^- is an inner filter effect.



Note that $\text{O}_2^{\cdot-}$ may also react with $\cdot\text{NO}_2$ to produce O_2 and NO_2^- (reaction 7). From the material balance it follows that the total amount of $\cdot\text{OH}$ radicals must equal that of $\cdot\text{NO}_2$. In the presence of 2-propanol each $\cdot\text{OH}$ radical is converted into $\text{O}_2^{\cdot-}$. Reaction 11 produces excess $\text{O}_2^{\cdot-}$ beyond the amount of $\cdot\text{NO}_2$. The excess $\text{O}_2^{\cdot-}$, which is not removed by $\cdot\text{NO}_2$, must react with $\cdot\text{NO}$ to produce back the peroxyntirite since the competing $\text{O}_2^{\cdot-}$ dismutation reaction is orders of magnitude slower. The solid curve in Figure 3 represents the best fit calculated using $\Phi(2) = 0.102$, $\epsilon_{253.7}(\text{NO}_3^-) = 4.25 \text{ M}^{-1} \text{ cm}^{-1}$, $k_d = 1.3 \times 10^{-5} \text{ s}^{-1}$, and $\epsilon_{253.7}(\text{ONOO}^-) = 550 \text{ M}^{-1} \text{ cm}^{-1}$, where the latter value is in agreement with the literature one.²⁵

Photolysis at 205–300 nm Using the Xenon Lamp. At 253.7 nm the $\pi \rightarrow \pi^*$ and $n \rightarrow \pi^*$ transitions overlap. Therefore, we extended our study to a wider range of excitation wavelengths to measure $\Phi(\text{ONOO}^-)_{2\text{-propanol}}$ at pH 13 and $\Phi(\text{NO}_2^-)$ at pH 4.2–4.5 in the presence of 10 mM formate.

Photolysis of alkaline nitrate solutions with monochromatic light from the xenon lamp required longer exposure time compared to the low-pressure mercury lamp. Therefore, the calculation of $\Phi(2)$ should take into account the spontaneous decomposition of peroxyntirite according to eq 12. In this equation $[\text{ONOO}^-]_t$ is the measured concentration at a given irradiation time, t , I is the absorbed dose rate in einstein $\text{L}^{-1} \text{s}^{-1}$, and $k_d = 1.3 \times 10^{-5} \text{ s}^{-1}$ is the apparent rate constant for the decomposition of peroxyntirite at pH 13.

$$\Phi(2) = ([\text{ONOO}^-]_t / I) (k_d / (1 - e^{-k_d t})) \quad (12)$$

The dependency of $\Phi(1)$, $\Phi(2)$, and $\Phi(\text{NO}_2^-)$ on the excitation wavelength is summarized in Table 1. The yields of nitrite at 205 and 214 nm with and without interference filters were, within the accuracy of the measurements, the same indicating that the scattered light is coming from long wavelengths where both iodide–iodate and nitrate solutions are optically transparent. The dependency of $\Phi(1)$ and $\Phi(2)$ on wavelength is also illustrated in Figure 4.

Madsen et al.⁶ reported that $48\% \pm 5\%$ of the nitrate molecules excited at 200 nm produce the cis isomer of peroxyntirite, $8\% \pm 3\%$ produce $[\text{NO} + \text{O}_2]^-$, and 44% decay to the ground state within 2 ps. $[\text{NO} + \text{O}_2]^-$ denotes $\cdot\text{NO} + \text{O}_2^{\cdot-}$ or $\text{NO}^- + \text{O}_2$, which probably recombine at longer time to form additional cis-peroxyntirite. If this is the case, the total yield of peroxyntirite should be $\Phi(2) = 0.56 \pm 0.08$,⁶ which is considerably higher than the value $\Phi(2) = 0.33 \pm 0.03$ presented in Figure 4. In addition, we observed the formation of $\cdot\text{OH}$ radicals with $\Phi(1) = 0.13 \pm 0.02$ at near 200 nm, which is evident from the effect of 2-propanol on the measured peroxyntirite yield at pH 13. In view of these observations it is tempting to suggest that the absorption spectrum observed at

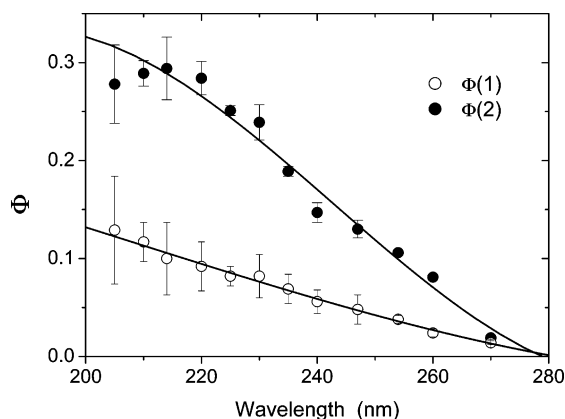
(25) Logager, T.; Sehested, K. *J. Phys. Chem.* **1993**, *97*, 6664–6669.

(26) Lo, W.-J.; Lee, Y.-P.; Tsai, J.-H. M.; Beckman, J. S. *Chem. Phys. Lett.* **1995**, *242*, 147–152.

Table 1. $\Phi(1)$, $\Phi(2)$, and $\Phi(\text{NO}_2^-)$ at Various Wavelengths

λ (nm)	$\Phi(\text{NO}_2^-)^a$	$\Phi(1)^b$	$\Phi(2)^c$
205	0.207 ± 0.011	0.129 ± 0.055	0.278 ± 0.040
205 ^d	0.222 ± 0.002		
210	0.198 ± 0.007	0.117 ± 0.020	0.289 ± 0.013
214	0.182 ± 0.005	0.10 ± 0.037	0.294 ± 0.032
214 ^d	0.175 ± 0.005		
220	0.172 ± 0.008	0.092 ± 0.025	0.284 ± 0.017
225	0.152 ± 0.005	0.082 ± 0.01	0.251 ± 0.005
230	0.149 ± 0.004	0.082 ± 0.022	0.239 ± 0.018
235	0.122 ± 0.010	0.069 ± 0.015	0.189 ± 0.005
240	0.097 ± 0.002	0.056 ± 0.012	0.147 ± 0.010
247	0.084 ± 0.002	0.048 ± 0.011	0.130 ± 0.009
253.7 ^e	0.065 ± 0.002	0.037 ± 0.004	0.102 ± 0.002
260	0.047 ± 0.002	0.024 ± 0.004	0.081 ± 0.002
270	0.0197 ± 0.0008	0.014 ± 0.002	0.0190 ± 0.0014
300	0.0094 ± 0.0002		$<0.002^f$

^a 0.02–1 M NO_3^- , 10 mM formate, pH 4.2–4.5. ^b $\Phi(1) = \Phi(\text{NO}_2^-) - 0.28\Phi(2)$. ^c 0.02–0.1 M NO_3^- , 20 mM 2-propanol, 0.1 M NaOH. ^d With interference filter. ^e Values taken from low-pressure mercury experiments. ^f Formation of peroxy nitrite was below the detection limit after 4 h of exposure to 4.42×10^{-7} einstein $\text{L}^{-1} \text{s}^{-1}$.

**Figure 4.** Dependency of $\Phi(1)$ and $\Phi(2)$ on excitation wavelength.

the femtosecond time range and attributed to the *cis* isomer⁶ contains a contribution from the *trans* isomer. The *trans* isomer is less stable and has not been reported in aqueous solutions. Measurements and calculations on KOONO in solid Ar matrixes show that the absorption maxima of *cis*-KOONO and *trans*-KOONO are at 325 and 375 nm, respectively,²⁶ but these results do not imply the same in aqueous solutions. We suggest that

the *trans* isomer may decompose into $\cdot\text{OH} + \cdot\text{NO}_2$ at a time scale longer than picoseconds and is responsible for the observed $\Phi(1) = 0.13 \pm 0.02$ in this study. In view of the error limits in the values of the different species and the uncertainty concerning the spectrum and extinction coefficient of the *trans* isomer in water, it is not possible to discuss the observations in quantitative terms of material balance. Decay of the *trans* isomer to nitrate may account for the apparent difference between the reported yield of picosecond peroxy nitrite of 0.56 and the sum of $\Phi(1) + \Phi(2) = 0.45$ in the present study, although the difference between the values is not outside the combined error limits.

Nitrate is one of the most common groundwater contaminants in the world, and its presence in the environment at elevated concentrations poses well-known human-health and ecological risks.^{27,28} The toxicity of nitrite is much higher as it oxidizes hemoglobin to methemoglobin, which cannot transport oxygen to the tissues. In the production of drinking water, UV light is increasingly being used for disinfection, posing concern about photolytic nitrite production from nitrate.

Figure 4 and Table 1 show a steady increase of the level of photochemical nitrite as the excitation wavelength of nitrate decreases below 300 nm. These results can serve the calculation of the expected nitrite yields in UV disinfection and decontamination. In practice, the yield of nitrite significantly decreases at low pH in the absence of organic contaminants as shown previously⁵ for excitation at 228 and 254 nm. In addition, bicarbonate, which is frequently present in natural water, lowers the yield of nitrite because CO_2 catalyzes the decomposition of ONOO^- into NO_3^- . Hence, in view of the polychromatic emission spectrum of medium-pressure light sources, which are often used in commercial reactors, the question of nitrite formation must be carefully addressed in relation to the pH of the water, concentration of inorganic and organic carbon, and spectrum and light intensity.

Acknowledgment. This research was partially supported by a Grant from the Israel Science Foundation of the Israel Academy of Sciences.

JA073609+

- (27) Fan, A. M.; Steinberg, V. E. *Regul. Toxicol. Pharmacol.* **1996**, *23*, 35–43.
 (28) Galloway, J. N.; Aber, J. D.; Erisman, J. W.; Seitzinger, S. P.; Howarth, R. W.; Cowling, E. B.; Cosby, B. J. *BioScience* **2003**, *53*, 341–356.